M. P. Manahan,[1] *A. E. Browning,*[1] *A. S. Argon,*[2] *and O. K. Harling*[2]

Miniaturized Disk Bend Test Technique Development and Application

REFERENCE: Manahan, M. P., Browning, A. E., Argon, A. S., and Harling, O. K., **"Miniaturized Disk Bend Test Technique Development and Application,"** *The Use of Small-Scale Specimens for Testing Irradiated Material, ASTM STP 888,* W. R. Corwin and G. E. Lucas, Eds., American Society for Testing and Materials, Philadelphia, 1986, pp. 17-49.

ABSTRACT: The objective of miniaturized specimen technology is to enable the characterization of mechanical behavior while using a greatly reduced or minimum volume of material. The significance of this technology is obvious to the nuclear industry where neutron irradiation space is limited and irradiation costs scale with specimen volume. In addition, the substantial advantages resulting from application of this technology in nonnuclear industries are only beginning to be realized.

The initial development of a miniaturized disk bend test (MDBT) for extraction of post-irradiation mechanical behavior information from disk-shaped specimens no larger than transmission electron microscopy samples is described. Central loading with a hemispherically tipped punch is used to measure load/deflection curves to fracture. These load/deflection curves are simulated using finite element analysis. This approach to miniature mechanical property testing is shown to offer the potential for the derivation of uniaxial flow properties.

This paper primarily emphasizes the development of test techniques and procedures; however, results for the determination of uniaxial tensile behavior are presented to demonstrate the validity of the basic methodology. Recommended techniques for specimen design, specimen preparation, experimental design, experimental implementation, and data analysis are presented.

KEY WORDS: mechanical behavior, miniature specimens, uniaxial tensile behavior, scanning electron microscopy, microstructure, continuum mechanics, finite element method, electrical discharge machining, lapping

[1]Senior Research Scientist, and Candidate for M. S. at the Ohio State University, respectively, Battelle Columbus Laboratories, Columbus, OH 43201.

[2]Professor of Mechanical Engineering and Director of Nuclear Reactor Laboratory, respectively, Massachusetts Institute of Technology, Cambridge, MA 02139.

The primary focus of this paper is on the development of the Miniaturized Disk Bend Test (MDBT) techniques for the determination of uniaxial tensile behavior, and many of the techniques and procedures discussed should be applicable to a wide variety of miniature specimen applications. Actual test results are presented only to help illustrate the validity of the methodology. In this paper we document the initial development of the MDBT which was carried out at MIT and some further work done at Battelle-Columbus. In doing this we have borrowed extensively from our previous publications [*1-4*], including the figures and tables used here. The results of continuing work at MIT are the subject of another paper presented at this symposium [*4a*].

The problem to be addressed is that of determining mechanical behavior from specimens which are substantially smaller than the conventional specimens currently in use. The initial impetus for the development of miniaturized specimen technology (MST) came from the need to test irradiated materials using as little material as possible. This is desirable because neutron irradiation space for materials investigations is limited and costly. In addition, in many future fusion reactor alloy development irradiations, such as those to be conducted in the Rotating Target Neutron Source (RTNS)-II facility and potentially in the Fusion Materials Irradiation Test (FMIT) facility if ever built, it will only be feasible to irradiate miniature specimens. It was recognized from the outset that MST would be applicable to materials investigations both in nuclear technologies and in non-nuclear technologies requiring mechanical behavior characterization from a very small volume of material (e.g., failure analysis and rapid solidification technology).

Research to date [*1-4*] at MIT on miniature tensile behavior determination has been primarily focused on disk-shaped specimens (nominally 3.0 by 0.25 mm) which are no larger than those used for transmission electron microscopy. Figure 1 graphically depicts the size scale involved by comparing miniaturized disk bend test (MDBT) specimens with a more conventional small post-irradiation uniaxial tensile specimen. These MDBT specimens are generally about 500 times smaller than the more conventional uniaxial tensile specimens currently used for post-irradiation testing, and about an order of magnitude smaller than most miniaturized tensile specimens. Since MDBT specimens are quite small, a nonstandard loading configuration is used. As a result, finite element analysis must usually be performed to convert the experimentally determined central load/deflection curves into stress/strain and other useful engineering information.

There are three principal conceptual innovative aspects inherent in our solution to the problem of obtaining mechanical behavior using miniature specimens:

1. Mechanical behavior specimens are used that are significantly smaller than those currently in use or that are significantly smaller than the in-service components from which they are cut.
2. An appropriate loading configuration is chosen to accommodate the

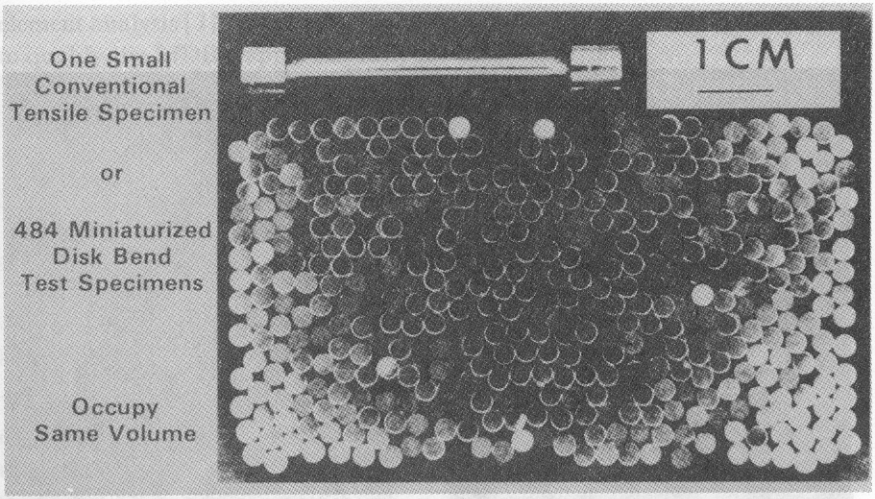

FIG. 1—*Miniaturized disk bend test specimens compared with one small conventional post-irradiation tensile specimen. The volume of one small tensile specimen is equal to the volume of 484 miniaturized disk bend test specimens.*

size scale involved or to represent the actual in-service loading. In practice, bending is used to extract mechanical behavior as opposed to the more standard approach of using uniaxial tension/compression loading requiring gripping extensions.

3. The finite element method is used to extract useful engineering information from the experimental data or to determine the desired experimental parameter ranges.

General Methodology

The recommended experimental configuration for miniature disk bend testing consists of a simply supported disk which rests in a cylindrical die and a hemispherical punch which presses the disk into the cavity as shown in the inset of Fig. 2. During the test, the applied load of the punch versus displacement under constant impression velocity is measured.

In order to analyze the MDBT using the finite element method, the boundary conditions must be accurately modeled. A new boundary condition model capable of analyzing intermittent frictional contact has been developed for this purpose [*1*]. The strain fields present in the MDBT are highly nonuniform, unlike the more conventional uniaxial tensile strain fields. Therefore precise three-dimensional boundary condition modeling is essential to set up the correct strain gradients in the plate. The model accounts for nonuniform strain as well as the nonlinear boundary conditions with shifting frictional contacts. The validity of the MDBT methodology has been examined for one material with well characterized mechanical behavior using small strain finite

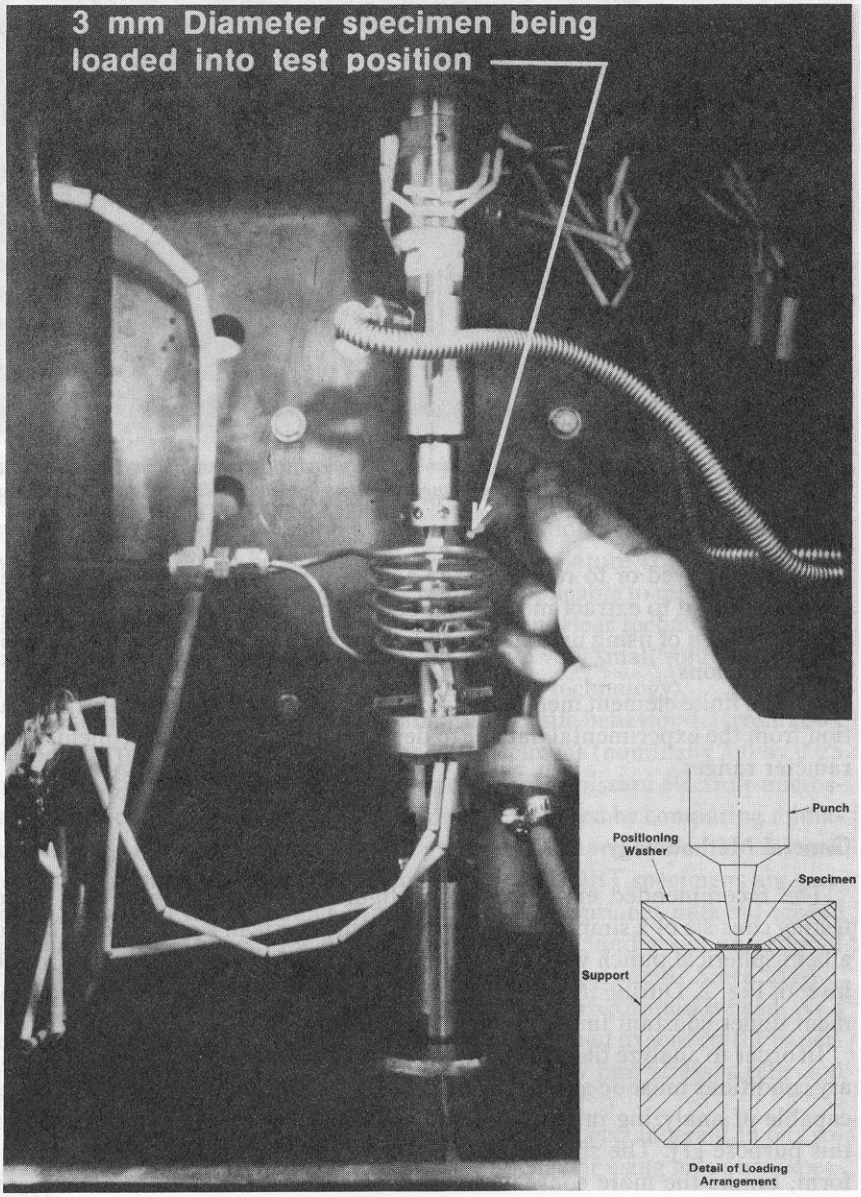

FIG. 2—*Actual miniaturized disk bend test apparatus installed in environmental chamber and schematic of miniaturized disk bend test section showing simply supported disk under central loading.*

element analysis [*1*]. While the results are promising, further tests are needed to qualify the MDBT approach fully for other materials.

The basic data inversion strategy for the near term for materials that behave isotropically is as follows:

1. Assume several flow curves that bracket the flow curve of the material being investigated.
2. Implement the finite element code and generate the central load/deflection curves for the various flow curves of Step 1.
3. Compare the finite element simulation of the experiment with the experimentally measured data. Repeat Steps 1 and 2 until a calculated central load/deflection curve falls within the experimental reproducibility band.

This procedure is illustrated in a flow chart format in Fig. 3. This is a near term strategy because in time the finite element data base will become sufficiently large, for a standardized specimen and loading geometry, that no further finite element runs will be necessary for a given material. Therefore an alternative fourth step would be:

4. Interpolation of calculated load/deflection curves for a measured load/deflection curve to determine the stress/strain curve of the material being tested.

The primary advantage of using finite element analysis for data inversion, as opposed to small strain analytical equations, is that the deformation response of the material can be measured for materials that exhibit large strains to fracture (i.e., ductile versus brittle materials). Also, in many geometries, finite element analysis is the only method of analysis available capable of dealing with complex loading problems. In general, the finite element method is much more versatile and appropriate than small strain analytical methods; therefore incorporation of the finite element method into the miniature specimen test methodology produces a far more powerful tool.

This section provides the background and overview for the MDBT. The following sections of the paper discuss specific aspects of the test.

Specimen Design Considerations

In choosing the specimen size and loading configuration for the determination of tensile behavior using the MDBT, careful consideration must be given to several important factors, such as:

1. Scale of material microstructure.
2. Behavior approaching that of a continuum in all directions.
3. Amount of material or irradiation space, or both, available.
4. Desired stress state during the test.
5. Plastic instabilities.

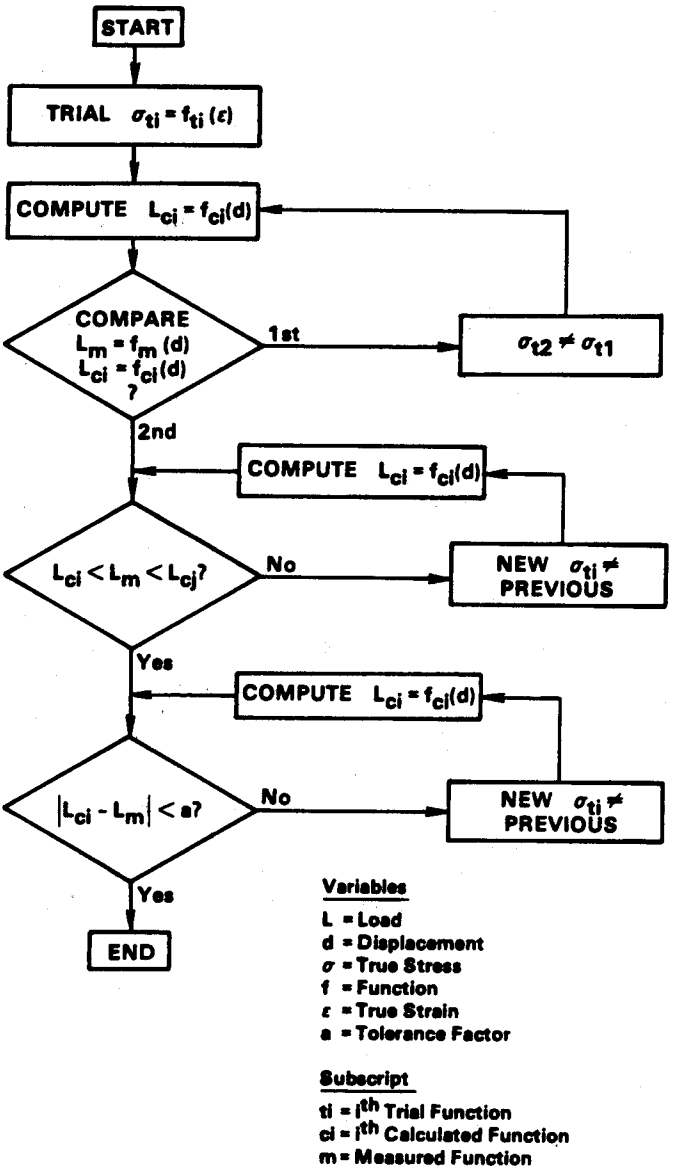

FIG. 3—*Flowchart of the basic data inversion strategy.*

The first step in any miniature mechanical behavior specimen design is to characterize the material microstructure. The key information to be determined includes variables such as average and maximum grain sizes, average and maximum particle sizes, and degree of anisotropy. All the microstructural variables are then analyzed to determine the minimum volume and smallest dimension sufficient to satisfy continuum behavior in all directions. In large strain deformation problems precise criteria for a minimum dimension to justify continuum treatment are difficult to give since they depend on the imposed constraints, the degree of texture evolution, etc. A desirable criterion might be that the minimum dimension be no less than ten times the largest microstructural heterogeneity. Since MST was originally developed to test samples prepared from small lots of material or for irradiation studies, the next step is to ensure that the continuum requirements do not violate the practical limits of the application. The desired stress state in the specimen during the test must be considered so that the optimum loading configuration can be adopted. Often it is desirable to simulate the anticipated in-service loading conditions to obtain data which are more representative of the final in-service application of the material. Plastic instabilities will be considered in detail in the following section.

As a result of these considerations, we chose a simply supported disk 3 mm in diameter and 0.25 mm thick to test irradiated fusion first-wall candidate alloys. A biaxial stress field was achieved by loading the disks transversely using a hemispherical punch.

Specimen Preparation Techniques

Specimen Machining

Because of the small size of the specimens, accurate machining which will not introduce any extraneous stress or bending is critical. There are various means of machining the specimens, depending on the form of the product available. Disks can be extracted from a plate by stamping or by turning down a small diameter rod and subsequently slicing disks from the rod. Various methods of cutting, from coarse saw blades and fine-blade cut-off wheels to electrical discharge machining (EDM), can be used to slice the disks.

In previous studies [*1*], specimens were prepared using ingot and rapidly solidified materials. The material chosen to test the validity of the MDBT concept was 316 stainless steel (SS) with 20% cold-works (CW) obtained in 0.348-mm-thick rolled sheet.[3] The specimens were stamped to a diameter of 3.000 ± 0.0076 mm and were subsequently precision lapped to a thickness of 0.2540 ± 0.0025 mm. Precision machine lapping was performed to ensure

[3]Material obtained from Hanford Engineering Development Laboratory (HEDL), heat designation 87210, otherwise known in the breeder reactor development program as HEDL N-LOT.

that the desired specimen thickness was achieved uniformly across the diameter of the specimen.

Rapidly solidified materials were provided in rod form [5]. The rods were cut in half and one rod for each alloy was cold swaged to obtain a 20% reduction in area. The six rods were then turned down to a diameter of 3.000 ± 0.0127 mm. Specimens of 0.381 mm thickness were cut using a high speed, water-cooled, silicon carbide blade and were subsequently precision lapped to 0.2540 ± 0.0025 mm thickness. These alloys were chosen for irradiation testing.

All cutting methods produce a layer of disturbed metal on the surface of the machined part. In the case of miniature disks, this layer can be a large percentage of the material involved, and the mechanical response can be significantly altered by the presence of this disturbed layer.

A study [6] has been conducted to determine the extent of the disturbed layer produced by various cutting processes. Other studies [7,8] which confirm the findings reported in Ref 6 have been conducted. A standard fine-blade cut-off wheel can produce as much as a 0.6-mm-thick layer of damage near the surface. Precision lapping is the recommended procedure to eliminate this layer; however, this can be a slow and costly process when a great deal of material must be lapped off or when the specimens in the lap batch are of widely differing thicknesses.

Recently, the alternative method of traveling wire EDM cutting has been investigated. Traveling wire EDM [8] is an extremely accurate cutting process. The recast layer is typically on the order of 0.005 to 0.008 mm thick [8], depending on the material and cutting conditions, which is much less than the 0.6 mm of disturbed metal produced by a cut-off wheel. Since these layers of disturbed metal caused by EDM are small and the cut edges are very flat and parallel, a shorter and therefore less expensive lapping procedure is required. The EDM/lapping technique was implemented to demonstrate its superiority over other methods. In addition to the recast layer created during the EDM cutting, there is also a heat-affected zone (HAZ) adjacent to the recast layer. The HAZ thickness is approximately the same as the recast layer for steels. Both layers must be removed by lapping.

A 152.4-mm-long, 12.7-mm-diameter rod was turned down using a piece cut from a 127-mm-thick plate of 304L stainless steel. This rod was then sliced by traveling wire EDM to produce 1.9558 ± 0.00254 mm thick disks. They were then precision lapped to 1.8872 ± 0.00254 mm. A thickness of 0.0686 mm was lapped off and a substantial time saving was realized because all the disks had nearly the same thickness and were already very flat.

The EDM process results in a cratered surface (Fig. 4). Figure 5 shows the recast layer using scanning electron microscopy (SEM). Micrographs taken after lapping showed that the lapping procedure is quite effective in removing the recast and HAZ layers and in producing the desired specimen dimensions with sufficient accuracy.

Another useful method for proving that the disturbed metal was eliminated

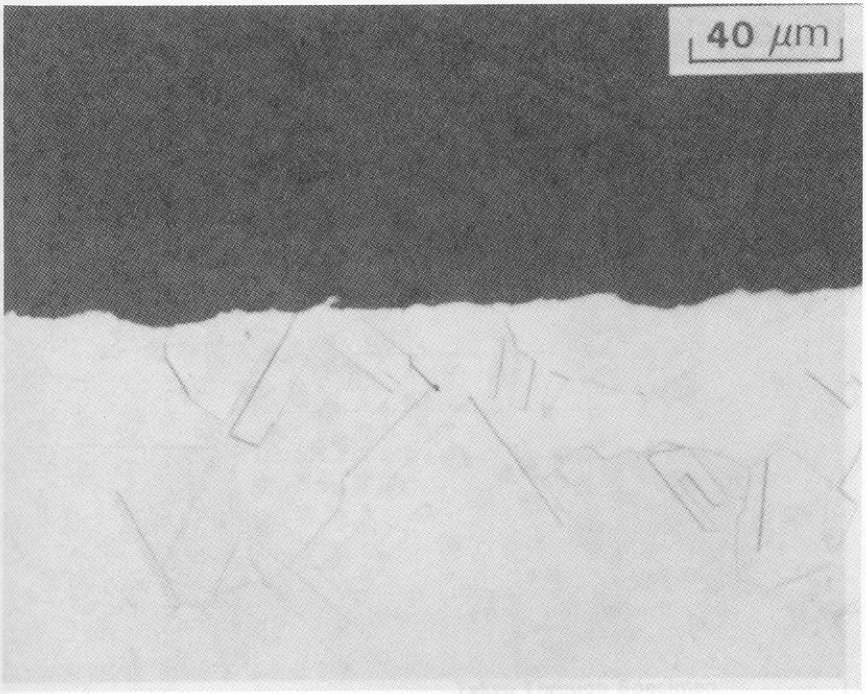

FIG. 4—*A light micrograph showing EDM cratered cut surface profile.*

is to measure the microhardness of the various layers. A disk was sectioned, mounted, and polished, and microhardness measurements were taken at various distances from the EDM cut edge. The result is shown in Fig. 6. A lapped disk was then tested in a similar fashion. Microhardness readings representative of the parent metal region were obtained for the near surface of the lapped specimen. This further verifies the successful minimization of the disturbed layers by lapping.

Although Knoop microhardness measurements can be performed in intervals of as little as 0.0254 mm, hardening due to plastic flow does occur in the immediate surrounding regions and will affect the results. Therefore, to attain the results in Fig. 6, microhardness measurements were taken at 0.0127 mm intervals or greater (depending on the material and indenter load) from the specimen edge through the thickness, while staggering the location parallel to the cut edge.

Specimen and Test Parameter Variations

Experiments were performed to assess the ability of the MDBT to resolve strain rate effects. In general, important strain rate dependence is observed

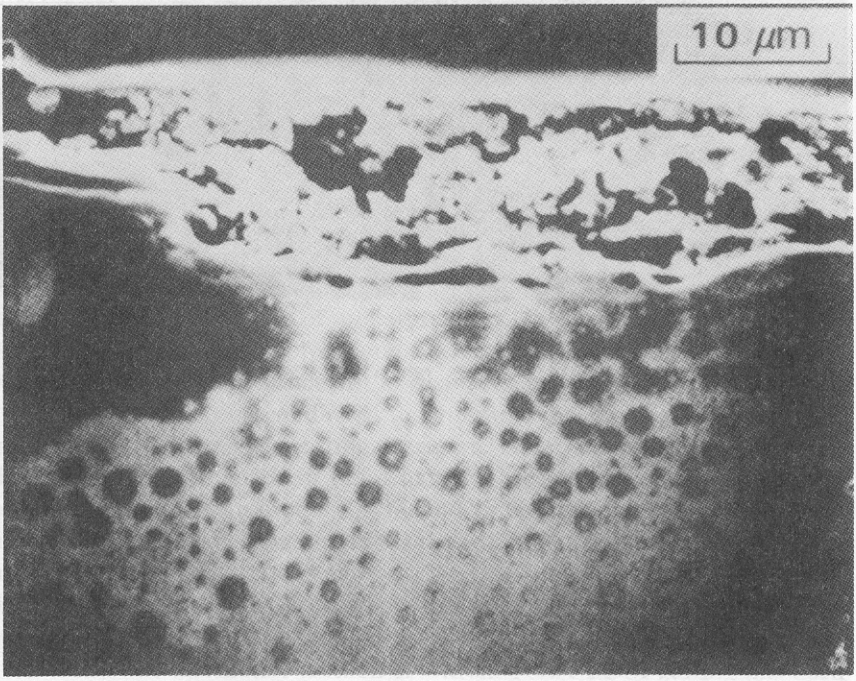

FIG. 5—*Scanning electron micrograph showing an EDM cut surface.*

only at high temperatures and low strain rates. For 316 SS, Paxton [*9*] reported negligible strain rate dependence for strain rates in excess of about 10^{-3} s^{-1} at 650°C. This behavior is shown in Fig. 7 for this material for Curves 1 to 4 at 500°C. The ability of the MDBT to clearly resolve strain rate effects, when they are present, is demonstrated by comparison of Curves 5 and 6 at 650°C with Curves 1 to 4 at 500°C.

For uniaxial tensile testing, the strain rate is clearly defined and is directly proportional to extension velocity. In the MDBT, however, the nonuniform biaxial stress field makes it impossible to obtain a simple analytical formula relating velocity to local instantaneous strain rate. Also, the instantaneous strain rate varies throughout the plate as the deformation proceeds.

In the MDBT experiments, an approximate definition of average strain rate was adopted:

$$\bar{\dot{\epsilon}} \simeq \frac{\Delta\epsilon_u}{\Delta t_u} = \frac{(\Delta\epsilon_u)v}{w_u} \tag{1}$$

where

$\bar{\dot{\epsilon}}$ = average MDBT strain rate,

Δt_u = time to reach maximum central load,

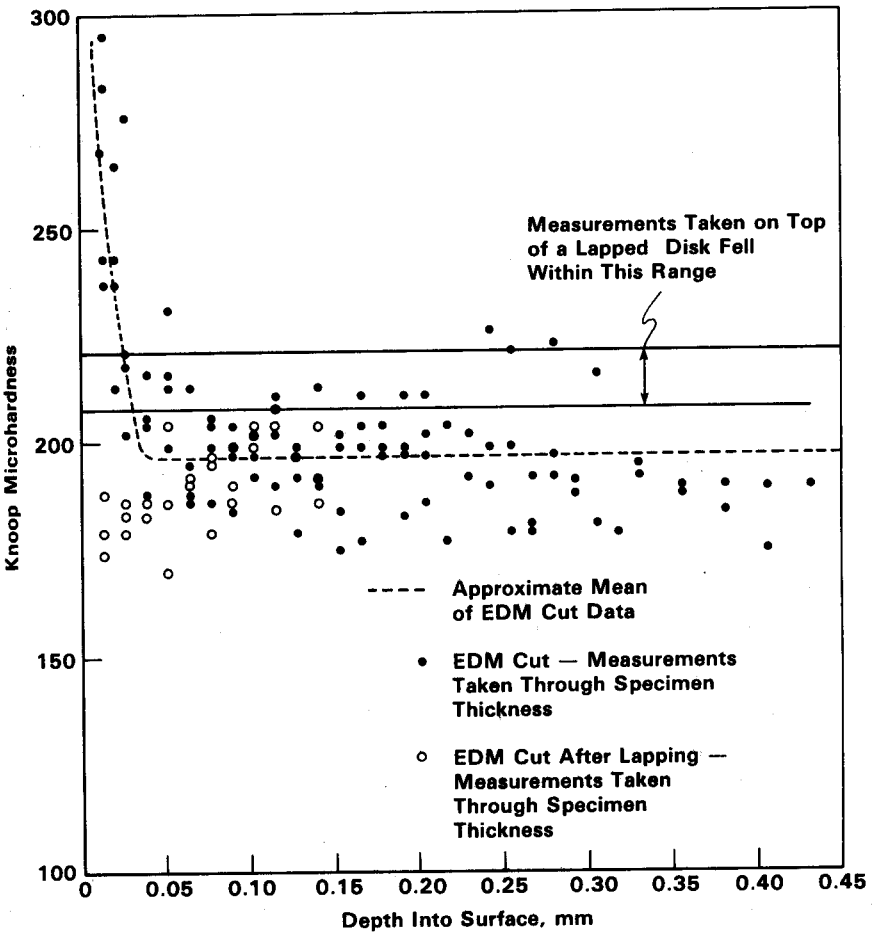

FIG. 6—*Knoop microhardness as a function of depth measured from specimen outer edge.*

v = punch velocity,
w_u = central deflection at maximum load, and
$\Delta\epsilon_u$ = equivalent biaxial strain under the hemispherical punch at the load maximum.

The average strain rates reported in Fig. 7 for the 20% CW 316 SS were obtained by this procedure.

Another parameter of interest is the aspect ratio (AR) of the specimens, defined as the diameter-to-thickness ratio. This was varied by changing the thickness and holding the diameter and all other experimental variables constant.

Large-AR-variation tests were performed to assess the range of AR's that could be tested using the MDBT procedure. For data inversion purposes, it is

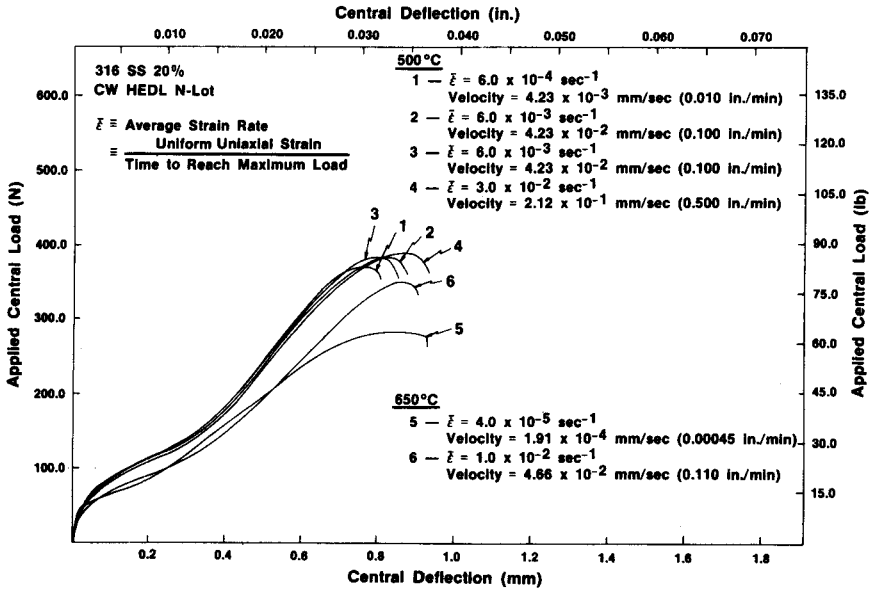

FIG. 7—*Demonstration of miniaturized disk bend test ability to resolve strain rate effects.*

preferable to standardize the specimen dimensions so that a large finite element data base can be developed. However, it is possible that some material processing conditions or irradiation space limitations may necessitate a change in specimen size.

Figure 8 presents the results for 302 SS specimens with AR's varying from 11.8 to 118.0. A plastic wrinkling instability was discovered for an AR of 118.0 as evidenced by the rapid load drop for Curve 1 in Fig. 8. Figure 9 shows the radial wrinkle that developed at the point of instability. Another specimen with an AR of 118.0 was loaded to a level short of the buckling load as shown in Curve 7 of Fig. 8. There was a permanent deformation in the specimen but no radial wrinkle present. Further evidence that the observed phenomenon is a plastic instability was obtained by testing a specimen with an AR of 59.0 at 500°C. No instability phenomena were observed. Therefore it was concluded that the MDBT procedure is reliable and applicable for specimens with AR's of less than about 60.0.

The variation of specimen thickness was investigated to assess exactly what machining tolerances result in acceptably small effects on the experimental data. The specimens used were 316 SS with a 3.0 mm diameter and were precision lapped to a thickness of 0.254 mm. These specimens were subsequently hand lapped on one side to provide for small thickness variations. The specimens were tested with the hand lapped side facing the punch. It was discovered that thickness variations of ± 0.0051 mm produce central load/

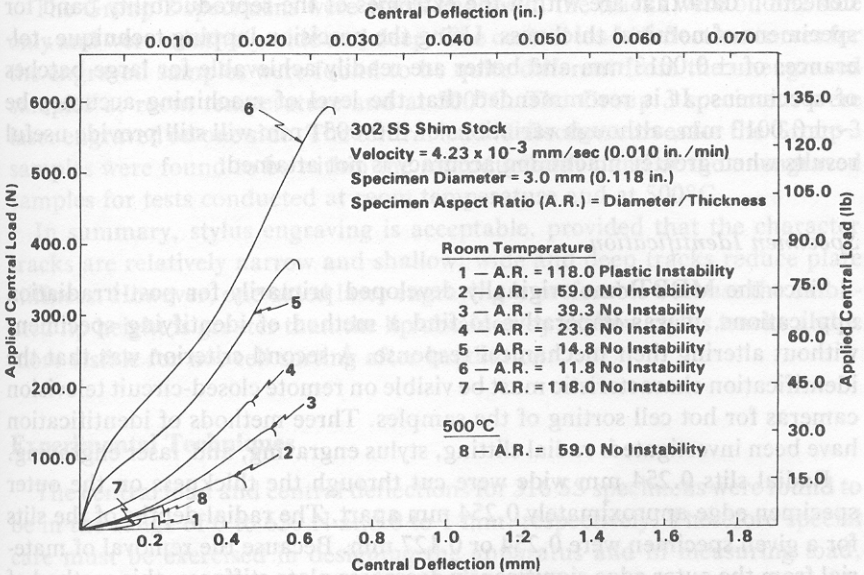

FIG. 8—*Large aspect ratio parametric investigation.*

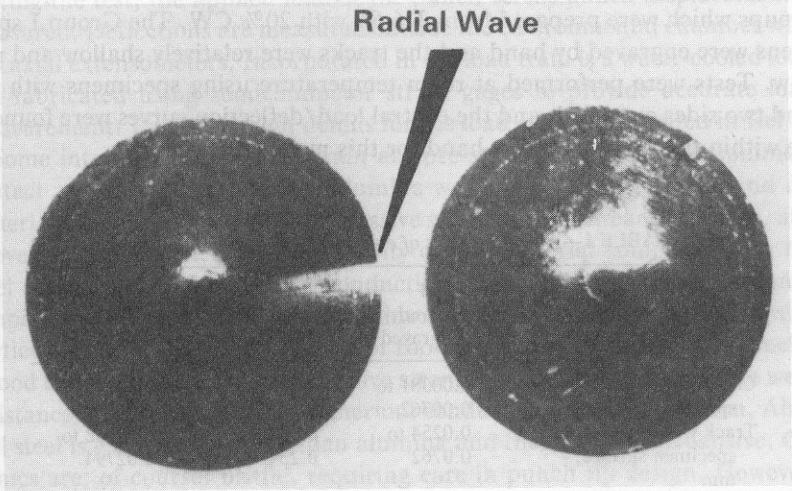

FIG. 9—(left) *Plastic wrinkling instability resulting in a radial wave for 302 SS specimen with aspect ratio of 118.0 tested at room temperature.* (right) *Axisymmetric deformation for 302 SS specimen with aspect ratio of 59.0 tested at room temperature.*

deflection data that are within the extremes of the reproducibility band for specimens of nominal thickness. Using the precision lapping technique, tolerances of ± 0.0013 mm and better are readily achievable for large batches of specimens. It is recommended that the level of machining accuracy be $\sim \pm 0.0013$ mm, although variations of ± 0.0051 mm will still provide useful results when greater machining accuracy is not attained.

Specimen Identification

Since the MDBT was originally developed primarily for post-irradiation applications, it was imperative to find a method of identifying specimens without altering their mechanical response. A second criterion was that the identification characteristic must be visible on remote closed-circuit television cameras for hot cell sorting of the samples. Three methods of identification have been investigated: radial slitting, stylus engraving, and laser engraving.

Radial slits 0.254 mm wide were cut through the thickness on the outer specimen edge approximately 0.254 mm apart. The radial depths of the slits for a given specimen were 0.254 or 0.127 mm. Because the removal of material from the outer edge significantly decreases plate stiffness, this method of identification was found to be unacceptable.

Another method of specimen identification that was examined is to engrave alphanumeric characters on one or both specimen surfaces. These identification processes can be quantified by measuring the height of the lip from the specimen surface, the width of the track at the specimen surface, and the depth of the track below the specimen surface. Table 1 lists measurements of these parameters made using an optical depth micrometer for three specimen groups which were prepared from 316 SS with 20% CW. The Group 1 specimens were engraved by hand and the tracks were relatively shallow and narrow. Tests were performed at room temperature using specimens with one and two sides engraved, and the central load/deflection curves were found to be within the reproducibility band for this material.

TABLE 1—*Characteristics of engraving tracks on specimens.*

Specimen Group Characteristic	1 Hand Engraved	2 Stylus Engraved	3 Laser Engraved
Character height from specimen surface, mm	0.00381 to 0.00762	0.0127 to 0.02032	0.03048 to 0.04572
Track width at specimen surface, mm	0.0254 to 0.0762	0.127 to 0.254	0.02032 to 0.02794
Track depth from specimen surface, mm	0.00381 to 0.01016	0.0127 to 0.03302	0.00254 to 0.00508

The Group 2 specimens were stylus engraved; the tracks were on one side only and were relatively wide and deep. The central load/deflection curves for the engraved samples were found to be quite different from the unengraved samples at room temperature and at 500°C. The Group 3 specimens were laser engraved on one side. The central load/deflection curves for the Group 3 samples were found to be within the reproducibility band of the unengraved samples for tests conducted at room temperature and at 500°C.

In summary, stylus engraving is acceptable, provided that the character tracks are relatively narrow and shallow; wide and deep tracks reduce plate stiffness. However, one-sided laser engraving is preferable because the exfoliated lip height is greater than the lip obtained by shallow stylus tracks and is more visible for hot cell sorting after irradiation.

Experimental Techniques

The central load and central deflections for 316 SS specimens were found to be in the range of 0 to 650 N and 0 to 1 mm, respectively. Therefore special care must be exercised in designing the apparatus and in measuring load, displacement, and temperature to ensure that accurate and reproducible data are obtained.

Apparatus Design

The test apparatus developed at MIT was adapted to an Instron 1331 servo-hydraulic machine with an environmental chamber and induction furnace. During the test, the applied load of the punch versus punch displacement is measured. Deflections are measured outside the environmental chamber with two axial extensometers. Incorporated in the load train is a water-cooled load cell fabricated using semiconductor strain gages to provide accurate load measurement. Further design details for the load cell are presented in Ref *1*.

Some interfaces in the load train are pre-stressed to minimize nonlinear contact responses. High density alumina was chosen for the punch and die material because of the large compressive strength, good wear resistance, and above all, the low thermal conductivity of this material compared with the steel specimens. If the thermal conductivity is too high, accurate specimen temperature control is difficult. Aluminum oxide is a good thermal insulator, particularly at high temperatures. For room temperature testing, tool steel is a good choice because the compressive strength is usually adequate, the wear resistance is reasonable, and the thermal conductivity is not of concern. Also, tool steel is easier to machine than alumina and therefore less expensive. Ceramics are, of course, brittle, requiring care in punch tip design. However, the compressive strength of high density alumina is sufficient to carry the loads present in the MDBT for hemispherical punch tip radii in excess of 0.254 mm, and the experiments verified this fact.

Alignment of the punch, die, and specimen is critical since disk stiffness increases with eccentricity of loading, and axisymmetry is desirable in the finite element analysis. Therefore it is recommended that great care be exercised when aligning the system. The usual alignment procedure consists of utilizing a fixture which will provide alignment of the punch and die axes of symmetry to within 0.0508 mm. Then the prepared, marked specimen is placed into the test position and a small load is applied. The location of the plastic indentation center can then be measured in an optical comparator and the appropriate correction for punch and specimen alignment made. In a similar fashion, the die alignment can be checked and appropriate corrective action taken. In this way, the punch, die, and specimen axes of symmetry can be aligned to within 0.0254 mm or better. The total eccentricity of loading for all experimental results reported herein was measured and found to be ~0.0178 mm. This eccentricity is well within the range which has been shown to produce acceptable experimental reproducibility bands [*1*].

Elevated temperature testing was carried out in an inert gas atmosphere to minimize oxidation and maintain good temperature control in the disks. Induction power was used to heat the samples through a susceptor after the environmental chamber was pumped down and flushed several times. Thermal contact between the metallic disk specimens and the alumina support is quite poor and varies throughout the deformation. This is why an inert gas blanket is necessary to provide a conductive heat transfer medium from the walls of the susceptor to the specimen. Argon gas was chosen because its thermal conductivity is approximately 2.5 to 9.0 times smaller than other inert gases considered. A low thermal conductivity gas was a reasonable compromise because its conductivity is high enough to heat the specimen, but still low enough to prevent significant heat loss to the walls of the chamber which were water cooled.

Three experimental parameters were varied to assess their relative importance in experimentation and modeling: (1) punch tip radius, (2) die diameter and support radius, and (3) punch friction coefficient.

Experimental evidence suggests that the specimen separates from the punch and leaves only an annular section of the plate in contact for a punch tip radius of 0.508 mm. In all experiments using this size punch, both at room temperature and elevated temperatures, the specimen became stuck on the punch tip after large plastic strains. The importance of accurately modeling the nonlinear boundary conditions present in the MDBT with the finite element method is further illustrated in Fig. 10, where the punch tip radius is varied while all other experimental variables are held constant. The 0.508 mm punch was adopted for all future tests because one MDBT criterion is the ability to perform fracture studies for ductile materials. The tests using the 0.762 mm radius punch are more closely related to bulge testing [*10*].

Likewise, the die diameter was varied and the central load/deflection curves were found to vary considerably, as anticipated. It was discovered during the finite element analyses that the through-thickness fiber rotations in

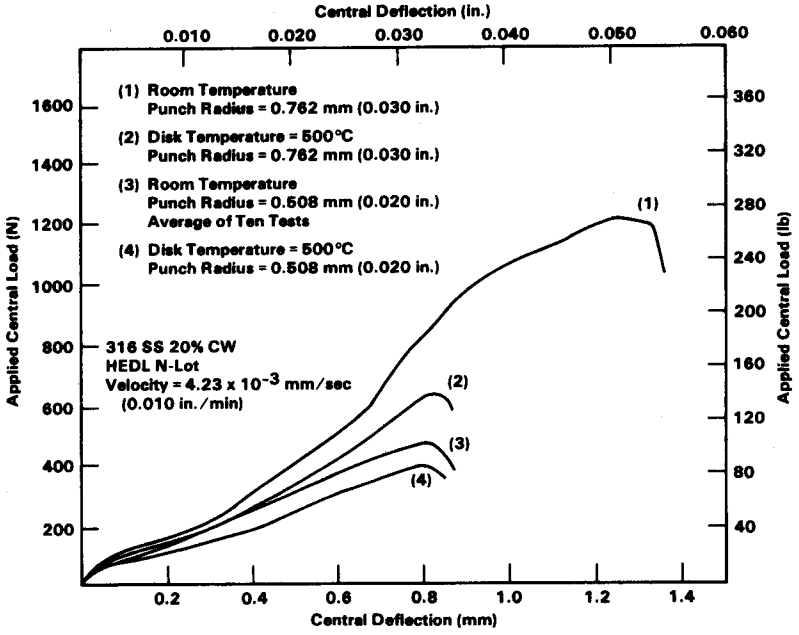

FIG. 10—*Miniaturized disk bend test experimental results for punch tip radius parametric investigation.*

the plate are initially much larger than the opposite tendency of the plate to draw into the die. This results in the plate bottom surface fibers being initially displaced radially outward. Therefore little die annular flat support thickness is required to support the plate properly. A reasonable die flat surface diameter of 2.46 mm was adopted for all subsequent experiments.

Figure 11 shows the effect of cleaning the punch tip with acetone between tests. The surface finish of the ceramics is porous, and metal from frictional sliding becomes entrained in the surface pores. Cleaning the tip between tests removes some of this material and thus increases the coefficient of friction slightly. This results in local plate stiffening near the punch tip, as evidenced by the increased load for a given central deflection over the last 0.40 mm of deflection. The punch tip should either be cleaned consistently or not cleaned for best reproducibility.

Data Analysis Techniques

Computational Methodology

Finite element analysis was performed to convert the experimental central load/deflection curves into stress/strain information that was used in turn for other evaluations such as ductility. In order to analyze the MDBT accurately,

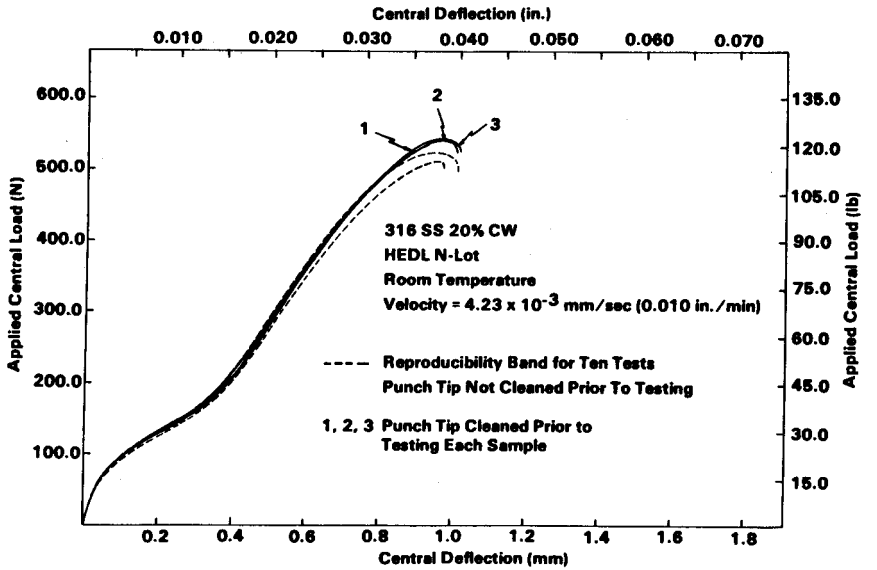

FIG. 11—*Effects of varying punch tip friction coefficient.*

a new finite element frictional contact boundary condition model has been developed [*1*]. The strain field present in the MDBT is highly nonuniform throughout the sample, unlike the more conventional uniaxial tensile strain fields which are constant in the gage section for a given static load up to the point of the necking instability. Therefore accurate three-dimensional boundary condition modeling is essential in simulating the actual strain gradients in the specimen during the experiment. The model used had the flexibility to cope with the non-uniform strain distribution and the shifting frictional contacts.

The ABAQUS [*11*] computer code was chosen for this modeling application because of its superior nonlinear capabilities. Small strain theory was used in all the analyses reported herein because at the time when the modeling study was performed large strain capability in ABAQUS was unavailable. Rodal has compared finite-strain theory with small-strain theory [*12*] for thin structures, such as beams, rings, and plates, and concluded that significant differences between the results of the finite-strain and small-strain theories develop only for strains greater than approximately 5.0%. These differences were found primarily in regions where large strain gradients occur. However, for high fluence post-irradiation materials investigations at elevated temperatures, the small-strain theory may prove adequate in many instances, since the ductility of many materials under these conditions is greatly reduced. Further work should be done with large strain theory and such work is in progress at MIT.

Demonstration of Validity of Methodology

All miniature specimen technology test approaches must be benchmarked before they can be safely used in practice. Furthermore, it is highly recommended that benchmark experiments be performed each time a miniature test is applied to a different material, even if the test methodology has been previously benchmarked. When miniature specimens are tested, material and test parameters must be considered that are of less concern, or even of minor importance, in conventional specimen testing. A benchmark experiment in this context consists of determining the desired mechanical behavior using large conventional specimens together with miniature specimens on material prepared from the same heat. The results of tests on miniature and large specimens are compared, and conclusions are reached concerning whether the miniature test is prototypical, sufficiently accurate, and reproducible.

Before discussing the benchmark results for miniature uniaxial tensile testing, a brief mention of the friction coefficient treatment is warranted. The friction coefficient for clean stainless steel on clean high density alumina lies between 0.2 and 0.6, and a value of 0.4 was used in all analyses reported herein. The mean coefficient of friction has been shown to be approximately temperature insensitive for temperature variations which merely affect the mechanical strengths of the two bodies [*13*]. This is because the ratio of the shear strength to hardness of the weaker material in contact is affected to about the same degree. Since the MDBT testing is done in an inert atmosphere, to first order, the assumption of no temperature dependence of the friction coefficient is valid. It is recommended, however, that the friction coefficient be treated as a tunable parameter. As mentioned in the Experimental Techniques section, it is essential that the experimental conditions, such as the friction coefficient, be held constant so that the experiment is reproducible. The finite element solution can then be adjusted by iterating on the friction coefficient until good agreement is obtained. The friction coefficient becomes particularly important at later stages of the deformation, when the punch and plate are in annular contact and the plate is displaced to the curved portion of the die. This occurs for deflections in excess of ~0.30 mm for stainless steel at elevated temperature. Since small strain theory was used, the accuracy of the solution was poor in this deflection range. Therefore tuning of the friction coefficient was not necessary. It is recommended, however, that the friction coefficient be tuned when using finite-strain theory.

The material chosen to benchmark the miniaturized uniaxial tensile test was 316 SS with 20% CW. The procedure followed was to test specimens prepared from the same heat of material as the large specimens. The known uniaxial tensile behavior at 482°C of the material [*9,14*] was used as code input. These data were piecewise linearized and a 20 element and 100 element mesh were run. The applied central load and deflection output is plotted with the experimental reproducibility band in Fig. 12. The finite element prediction is quite accurate up to a central deflection of about 0.45 mm. The force

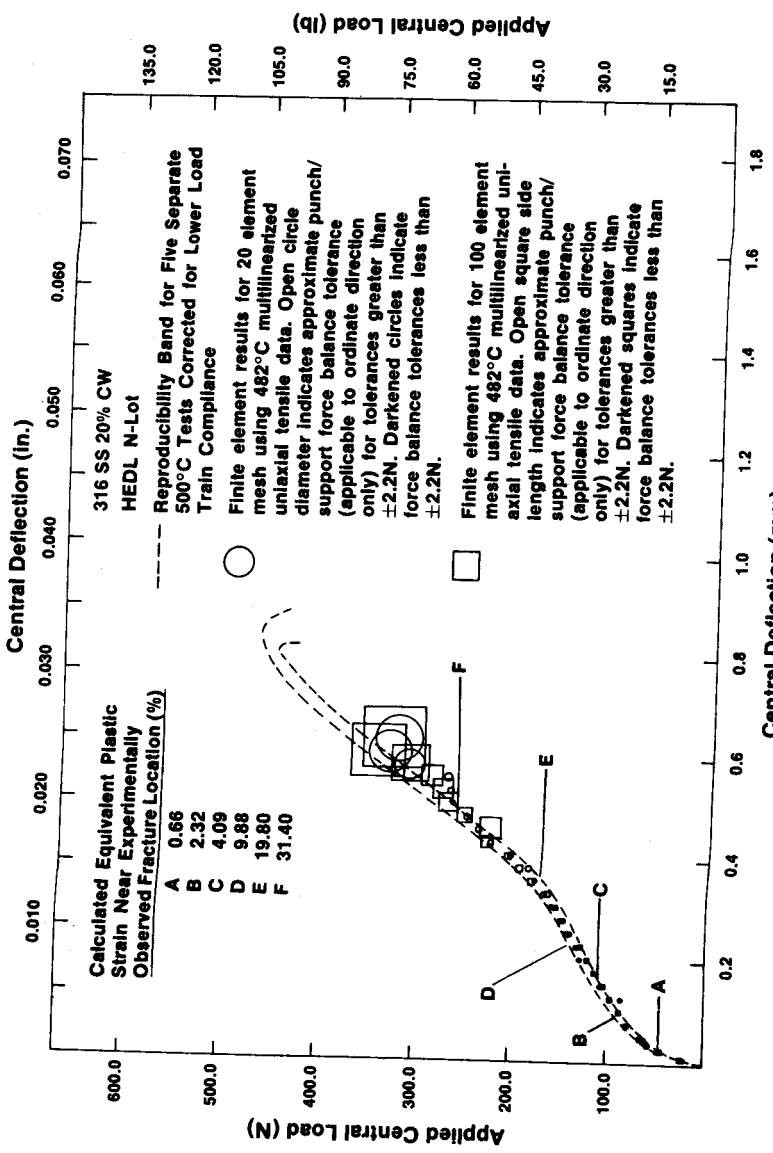

FIG. 12—*Demonstration of validity of miniaturized disk bend test methodology. Finite element solution generated using known uniaxial stress/strain behavior shows excellent agreement with miniaturized disk bend test data up to deflections of 0.45 mm.*

balance tolerance provides an estimate of the central deflection beyond which small strain theory is no longer valid. As shown, the convergence tolerance becomes sizeable after a central deflection of about 0.45 mm for the 100 element mesh. One of the bottom elements near the plate center actually turns in on itself at this deflection. This explains the large force balance tolerance for the 100 element mesh after central deflections of 0.45 mm. Since there are only two elements through the thickness for the 20 element mesh, this phenomenon occurs at a larger central deflection for this mesh. Therefore, as anticipated, for materials which exhibit large ductility, the finite strain theory is needed.

Accuracy of Experimental Data Inversion Technique

When using miniature specimens, it is advisable that analyses be performed and conclusions be drawn concerning the accuracy of the miniature specimen test and how it compares with large specimen testing. Analysis of the sources of error can lead to changes in the basic methodology which may result in better accuracy. In other cases, it may not be possible to improve the accuracy of a miniature specimen test beyond a certain level due to limitations inherent in the methodology or technique. It is recommended that miniature specimen tests be classified as either:

1. *Accurate test*—comparable accuracy with conventional specimen tests, or
2. *Screening test*—not of comparable accuracy with conventional specimen tests.

In order to implement this classification system, numerical values would have to be assigned to each test classification by ASTM. It is premature to assign these values now because too few data exist to ensure accurate statistics. However, a factor-of-1.5 increase in the 95% confidence band width of large specimens might be a reasonable criterion for defining an accurate miniature test. Likewise, a 95% confidence band width increase by a factor of 1.5 to 3.0 of large specimens might define the range where a miniature test would serve as a screening test. Error bands in excess of a certain prescribed level would invalidate a given miniature test methodology or possibly invalidate the use of a given methodology on certain materials.

An analysis was performed to gain understanding of the resolution capability of the MDBT methodology as compared to the more conventional approach of uniaxial tensile testing to determine mechanical behavior. The multilinearized work hardening curve for the 316 SS 20% CW material at 482°C was increased by 2% and 10%, respectively, for a given strain level. For ease of discussion, these two cases will be loosely referred to as the 2% flow stress input change and the 10% flow stress input change. The 20 element mesh was used to determine central load and displacement information.

The calculated central load/deflection curves were plotted along with the experimental reproducibility band. The results for the 0% flow stress input change and the 2% flow stress input change fell within the experimental reproducibility band. However, the calculated load/deflection curve for the 10% flow stress input change fell well above the experimental reproducibility band. Therefore the stress/strain resolution capability of the MDBT methodology in fitting the experimental load deflection curves for 20% CW 316 SS lies somewhere between a 2 and 10% flow stress input variation.

In order to gain a more quantitative understanding of the MDBT stress/strain determination accuracy, the percent change in calculated applied central load was plotted against the normalized central deflection for the 2 and 10% flow stress input changes. A 2% change in flow stress input results in a mean calculated load change of approximately 1.8%. Likewise, a 10% change in flow stress input results in a mean calculated load change of approximately 8.3%. These results are plotted in Fig. 13. The resulting curve is approximately linear and lies very close to the unity slope line, which indicates good inherent resolution capability for the MDBT methodology. If, for example, the slope of this line were significantly greater than 1.0, then a small change in the load response would result in a large difference in the calculated stress; consequently, a small experimental error would result in a large uncertainty in the calculated stress/strain results. Fortunately, this is not the case. The nearly linear response indicates that it is possible to obtain reasonable

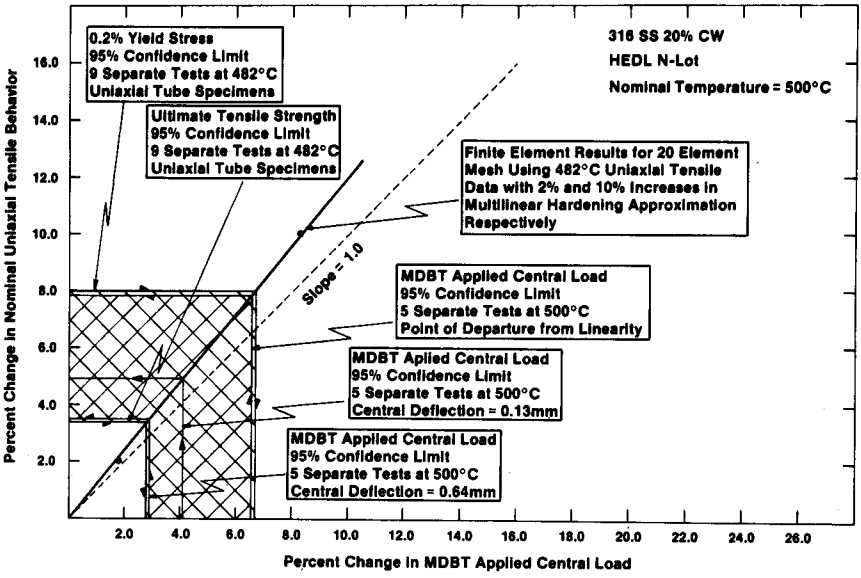

FIG. 13—*Uncertainty mapping function from uniaxial tensile stress space to miniaturized disk bend test applied central load space.*

accuracy in the MDBT stress/strain calculation, provided that the experimental error is sufficiently reduced.

Figure 13 can be thought of as an uncertainty mapping function, mapping uncertainty in uniaxial tensile stress into uncertainty in central load of the MDBT, or vice versa. Reference *9* reported 95% confidence limits for the 0.2% yield stress and ultimate tensile strength (UTS) of the 316 SS 20% CW material at 482°C for nine separate uniaxial tensile tests on tube specimens. The 95% confidence limit for the 0.2% yield stress was ±8.13% of the mean and the 95% confidence limit for the UTS was ±3.41% of the mean. Using Fig. 13, these 95% confidence limits in stress map into maximum calculated changes in MDBT mean applied central loads of ±6.8% and ±2.75%, respectively. As discussed in Ref *1*, 95% confidence limits for the MDBT applied central load were calculated at 500°C using the experimental data. The 95% confidence limit at the point of departure from linearity on the load/deflection curve was found to be ±6.69% of the mean. This point on the central load/deflection curve is primarily affected by the 0.2% yield stress. Further discussion of the interpretation of the central load/deflection curve will be presented later. At a central deflection of 0.64 mm, the 95% confidence limit was found to be ±2.85% of the mean. This point on the central load/deflection curve is primarily affected by the UTS. Again, using Fig. 13, these confidence limits are found to map into stress uncertainties of ±7.90% and ±2.50%, respectively. The confidence limit band width for uniaxial testing is primarily determined by material variability and experimental errors such as those introduced in specimen machining, gripping extensions, column alignment which can result in bending, and transducer accuracy. The confidence limit band width for the MDBT is primarily determined by material variability and experimental errors such as those introduced in specimen machining, friction coefficient variation, punch/die/specimen alignment, and transducer accuracy.

In summary, Fig. 13 indicates that the MDBT methodology is potentially capable of delivering uniaxial work hardening information with approximately the same level of accuracy as that present in the more conventional uniaxial tensile testing approach for 316 SS tested at elevated temperatures. In the future, more data should be taken to determine whether the conclusion holds for other materials and loading configurations as well. Also, the 95% confidence limits vary significantly with temperature for a given heat of material, and this effect should also be examined in future research. It is recognized that additional data inversion research is necessary. Nevertheless, these results on the MDBT uniaxial tensile resolution capability are quite encouraging.

As mentioned in the General Methodology section, it is desirable to develop interpolation software once the finite element data base is sufficiently large for a given material. This will enable data inversion without the need for relatively expensive finite element analyses. However, some additional uncer-

tainty would be introduced into the data inversion strategy using this approach.

Data Inversion Strategy

In general, the most effective way to implement the data inversion strategy is to use trial stress/strain functions that are expressible as mathematical relations. The simplest such mathematical relationship would be the bilinear hardening approximation. In this way, the shape of the trial stress/strain functions can be limited to a narrow class of shapes. The analyst must take care in choosing mathematical representations to ensure that the material being tested actually performs in accordance with the choice of the shape function. In particular, the post-irradiation shape function may not be similar to the pre-irradiation shape function. Also, computing costs can be reduced by taking advantage of prior knowledge regarding the shape and expected behavior after irradiation (e.g., irradiation hardening or softening behavior, ductility reduction.)

The flow curves of many materials from initial yield to the end of the region of uniform plastic deformation, and often beyond, can be approximated by a power law relation as follows:

$$\sigma = K\epsilon^n \tag{2}$$

where

σ = true stress,
ϵ = true strain,
n = strain-hardening exponent, and
K = strength coefficient.

The strength coefficient can be written in terms of the uniform stress and strain as follows:

$$K = \frac{\sigma_{\text{UTS}}}{n^n} \tag{3}$$

where σ_{UTS} = true ultimate tensile strength.

Therefore the entire flow curve can be parameterized by the true ultimate tensile strength and the true uniform strain. The yield stress is defined by cutting off the flow curve at 0.2% strain.

The elastic stiffness of the material is characterized by Young's modulus, which is structure insensitive in a quasi-homogeneous solid of constant composition because the atomic binding cannot be significantly altered without modifying the basic nature of the material. Therefore a new set of data inversion curves is needed whenever Young's modulus changes. Young's modulus

should be determined to sufficient accuracy by testing in accordance with ASTM standards. A pre-irradiation uniaxial test at temperature is advisable since the stress/strain curve generated usually provides a bound to the post-irradiation strain hardening or softening behavior.

A variety of materials [*1*] in the post-irradiated condition were tested for irradiation experiments carried out in the High Flux Isotope Reactor at Oak Ridge National Laboratory. The calculated irradiation parameters are listed in Table 2. The pre- and post-irradiation results for the primary candidate alloy/rapidly solidified (PCA/RS) material are shown in Fig. 14.

As discussed earlier, radial slitting can produce significant errors in the central load/deflection response. Therefore pre-irradiation tests on slitted specimens were performed for comparison. Unfortunately, the radial slitting

TABLE 2—*HFIR CTR-32 calculated irradiation parameters.*

In-Core Position	Temperature, (°C)	Fast Fluence ($E > 0.1$ MeV) (neutrons/m^2)	Thermal Fluence (neutrons/m^2)	Total Fluence (neutrons/m^2)	dpa (316 SS)	He (12.4% Ni) (atom. ppm)
4	600	1.1×10^{26}	2.1×10^{26}	4.4×10^{26}	8.5	360
9	500	1.1×10^{26}	2.1×10^{26}	4.4×10^{26}	8.5	360

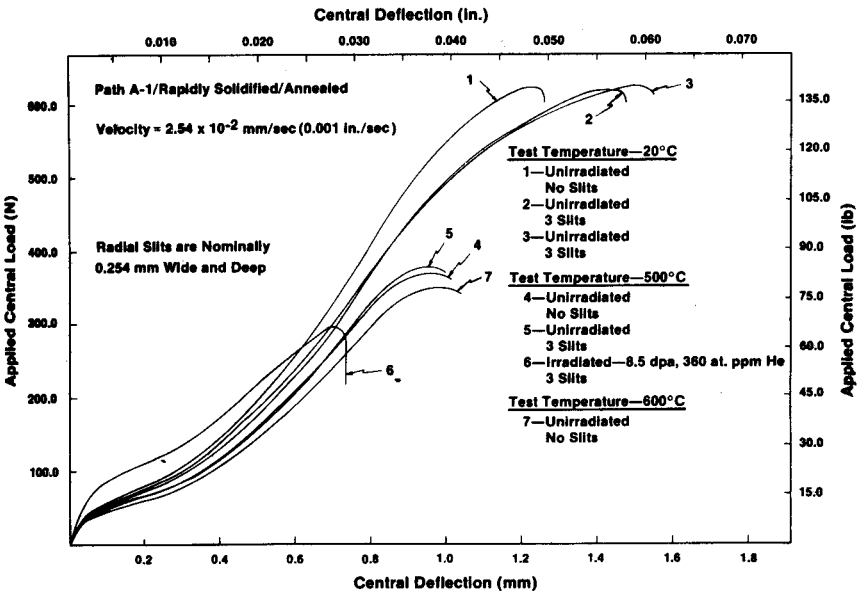

FIG. 14—*Pre- and post-irradiation data for PCA/rapidly solidified/annealed material.*

study results were not available before submitting the specimens for irradiation. Examination of Fig. 14 indicates that for the materials tested, the slits can produce significant effects on the central load/deflection response at room temperature. However, the effects are not as dramatic at elevated temperatures where the material flows more readily. Therefore, although not exact, the elevated temperature data for the post-irradiation samples are fairly close to data obtained for samples without radial slits.

In the analyses reported herein, the work hardening relationships before and after irradiation were assumed to be of the same shape. This assumption was shown to be reasonable for the materials examined [*1*], although this assumption will not necessarily hold in all cases. In future materials testing it will be useful to gain experience using some alternative phenomenological relations for the work hardening curves.

The parameterized spectrum of flow curves analyzed is shown in Fig. 15. The resulting central load/deflection curves generated using the various flow curves are presented in Fig. 16 with the post-irradiation experimental curves superimposed. The PCA/RS/20% CW experimental data are best matched

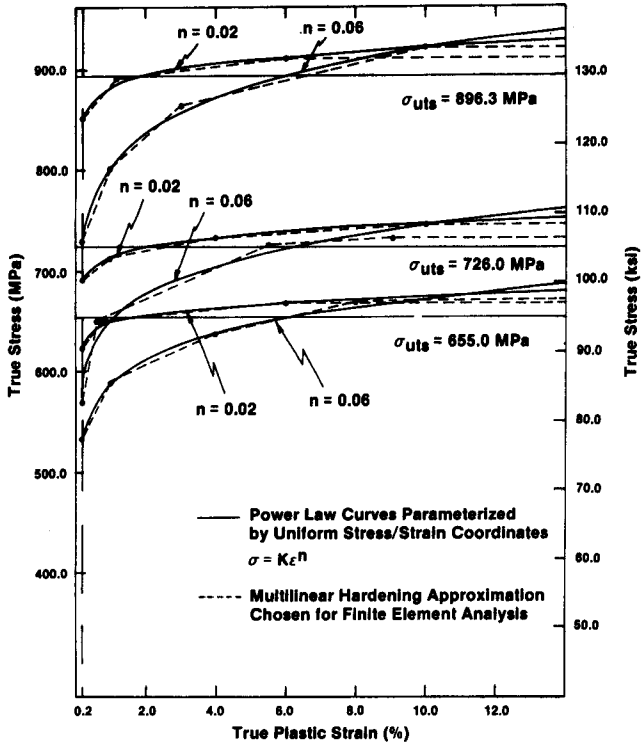

FIG. 15—*Spectrum of parameterized flow curves used to invert post-irradiation data.*

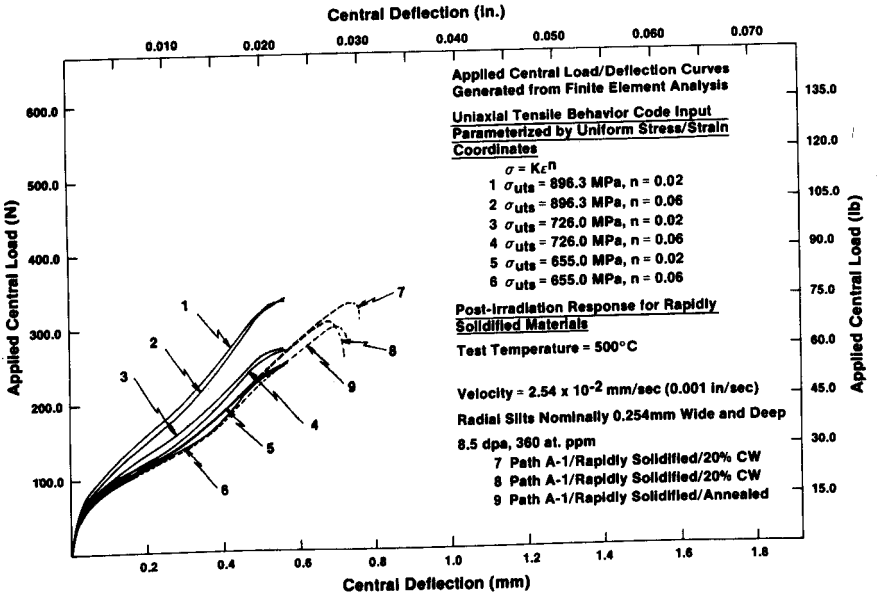

FIG. 16—*Post-irradiation data inversion of rapidly solidified materials using miniaturized disk bend test methodology.*

by Curve 5 and the PCA/RS/annealed experimental data are best matched by Curve 6. These results are only approximate because the slits in the irradiated specimens produced some experimental inaccuracies. There were only a few test specimens, and the calculated load deflection curves were obtained using small strain theory, which cannot be expected to provide a good fit when strains in excess of 5% are present.

Interpretation of Load and Deflection Data

Analyses were performed to provide a fundamental interpretation of the load and deflection data. As illustrated in Fig. 17, the central load/deflection curve can be divided into five distinct regions, each being governed by widely differing modes of deformation and phenomena.

Examination of the finite element strain contours reveals that the plate yields shortly after contact with the punch in a localized region near the punch tip. Yielding occurs next on the bottom of the plate due to bending. Over the initial linear portion of the load/deflection curve, which spans the first 0.0381 mm of deflection, most of the plate response is in the elastic regime. This has been verified in the finite element analyses and also experimentally by loading and unloading several times up to the point of departure from linearity on the load/deflection curve. During these experiments, the

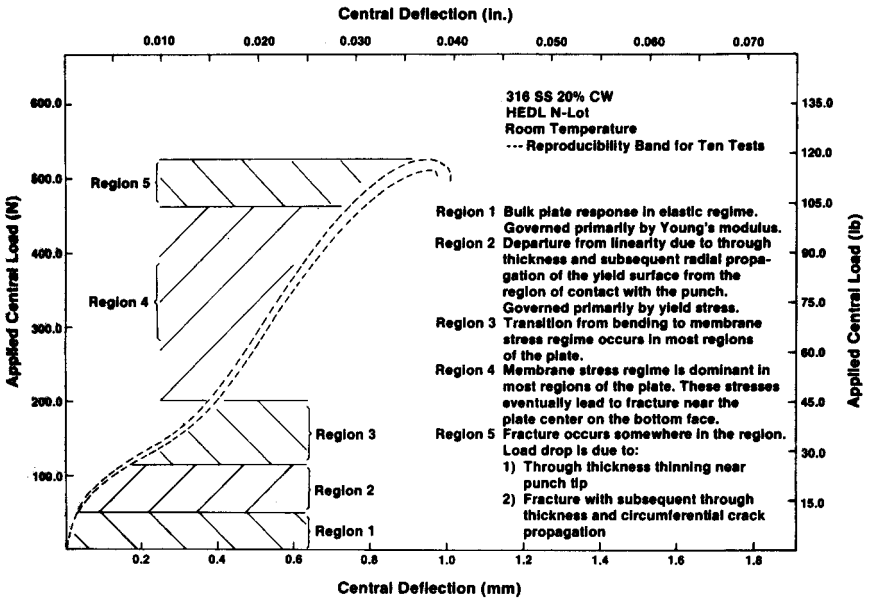

FIG. 17—*Fundamental interpretation of applied central load deflection curves for 316 SS 20% CW.*

linear portion of the curve was retraced until the plastic zone spread over large portions of the plate, resulting in a departure from linearity on the load/deflection curve. Also, a small plastic indentation at the center of the plate where the punch made contact was observed in this region of the load/deflection curve.

During the deformation in Region 1, the yield surface in the plate propagates through the thickness from the punch contact zone and radially outward over a cylindrical plate region approximately 0.18 mm in diameter. A similar yield surface propagates from the bottom of the plate opposite the punch. Thus Region 1 is governed by Young's modulus, the yield stress, and the initial hardening rate. The Region 2 departure from linearity is due to continued propagation of the yield surface in the plate radially outward but over much larger portions of the plate. In essence, large regions of the plate are yielding; thus Region 2 is governed primarily by Young's modulus, the yield stress of the material, and the hardening rate.

The ratio of the outermost fiber radial stress components on the top and bottom plate surfaces for two radial locations was plotted as a function of the punch central deflection to assess the range of central deflections over which the transition from bending to membrane stretching occurs. The transition occurs for central deflections between approximately 0.18 and 0.38 mm. Thus Region 3 illustrates the portion of the central load/deflection curve

where the transition from bending to membrane stretching occurs in most regions of the plate. In Region 4, membrane stretching is dominant in most regions of the plate. These stresses eventually lead to fracture in Region 5. The fracture occurs on the bottom of the plate near the center. An investigation to determine the approximate location on the central load/deflection curve where fracture initiates for 302 and 316 SS was performed. These results for 302 SS are shown in Fig. 18. For both materials, the fracture initiates prior to the load peak. Fracture has been observed to occur at a radial location of approximately 0.254 mm for the 302 SS shim stock specimens.

The load drop in the MDBT is actually due to two causes. The first is the through-thickness thinning of the plate near the punch that decreases the load carrying capacity. The second is fracture with subsequent through-thickness and circumferential crack propagation.

Since there are significant strain gradients present in the miniature disk, it is not, in general, possible to derive any stress or strain information directly from the load/deflection curve. It is recommended that finite element analysis be performed to convert the experimental data into stress/strain information.

Discussion

We have presented results on the development of a miniaturized specimen methodology to probe the mechanical behavior of irradiated alloys where the

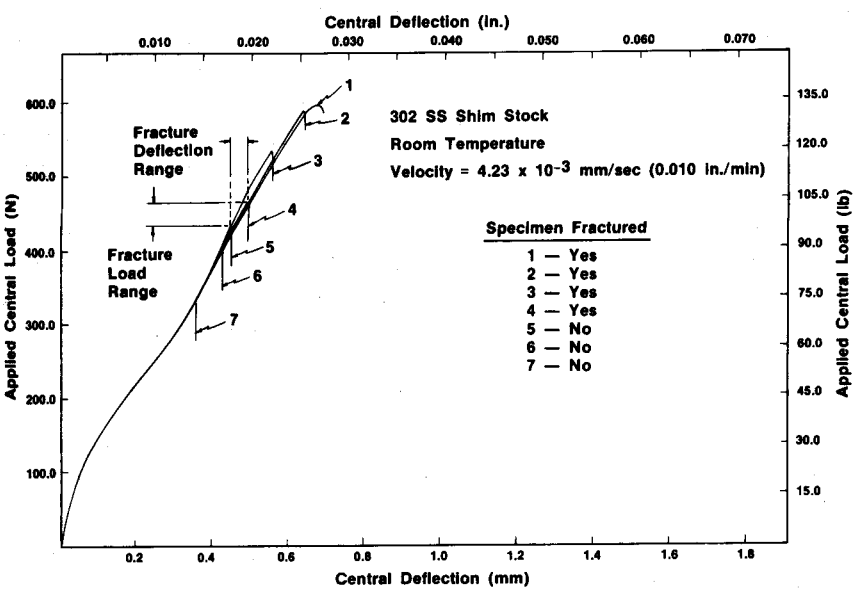

FIG. 18—*Results of fracture initiation investigation for 302 SS.*

amount of material that can be incorporated in irradiaton capsules is at a premium. In some respects, our test resembles a hardness test, but ours is superior because it requires much less material and can provide a measure of the entire stress-strain response of the alloy and some information on its fracture behavior as well. As with the hardness experiment, however, it is based on highly nonuniform deformations. It is clear that since the experiment is one in which the strains and strain gradients are monotonically altered and where steady-state deformation is never achieved, the interpretation of the results into usable stress-strain information requires finite element analysis procedures. A de-convolution of the force-displacement curves into stress-strain curves or creep response depends upon the type of material flow curve being examined and how the flow curve can be parameterized. A unique data inversion is possible for non-hardening materials for which the yield and fracture stress coincide. Also, isotopic material that can be adequately modeled by a bilinear hardening can be treated in a way that produces unique results. For some materials, however, several different stress-strain responses can give rise to similar force-displacement curves, and a unique deconvolution of the latter information into stress-strain curves or creep response is not possible. In these cases, the only acceptable approach, which we have also followed, is to consider a family of parameterized stress-strain responses and compute with these families the possible force-displacement responses which are then expected to bracket the actual observations. We have followed this procedure and recommended its usage. Furthermore, we are of the opinion that the level of precision of such interpolated stress-stain responses obtained from families of computed responses could furnish a very adequate means of evaluation of material response that can be used for comparative purposes. The level of precision should also be adequate for many applications in computational modeling studies. For more fundamental studies where comparison of different responses requires accurate evaluation of small differences in material behavior, and above all where material deformation instabilities are an essential part, only uniform strain field experiments will be acceptable.

We foresee many application areas for the MDBT also outside the field of nuclear materials development, such as in probing alloys in structures for assessment of remaining creep life, in failure analysis, and in alloy development in general where only very small amounts of material can be produced.

Summary and Conclusions

Based on experience in testing miniature disk-shaped samples at Battelle-Columbus and MIT, it is recommended that the following techniques and procedures be followed in miniature specimen testing:

1. Specimen design must begin with a careful characterization of the material microstructure. Particular care must be exercised to ensure that continuum behavior is maintained in all directions.

2. Specimen preparation depends on the form of product available. The recommended preparation procedure for miniature disks is to:

- Turn down a rod to the appropriate diameter.
- Slice the disks using traveling wire EDM.
- Precision lap the specimens to the desired thickness.

3. The variation of microhardness from the surface into the median plane for each material should be determined to characterize the thickness of disturbed material generated during cutting, and such disturbed layers should be removed by lapping.

4. Single-sided laser engraving is recommended as the specimen marking technique because the exfoliated lip height is readily visible in remote cameras for hot cell sorting and has been shown to have negligible effect on the specimen response.

5. Special care must be taken in aligning the punch, die, and specimen in the test apparatus, particularly if credit for axisymmetry in the finite element analysis is taken.

6. The specimen temperature must be carefully calibrated. The recommended practice is to solder a small-diameter thermocouple to the specimen and calibrate it relative to permanently embedded thermocouples in the disk support piece.

7. Finite element analyses, where appropriate, should be used for data inversion. Accurate boundary condition modeling must be employed in the analysis, particularly at the functional contacts. If multiaxial stress/strain response is desired, mesh refinement near the punch tip is necessary. Finite-strain theory should be used for the analysis of very ductile materials.

8. A benchmark experiment, which consists of comparing the results from testing the miniature and large specimens, should be performed for each mechanical behavior test. In addition, each time a given successful test methodology is applied to a new material, a benchmark experiment should be performed.

9. Conclusions concerning the accuracy of miniature specimen tests should be made for each benchmark experiment. In particular, miniature specimen tests should be classified as one of the following:

- *Accurate test*—comparable accuracy with conventional test method, or
- *Screening test*—not of comparable accuracy with conventional specimen test method, but yields useful data.

10. The use of finite element techniques to analyze the results of miniature disk bend tests has been shown to yield useful results. Further development of the data inversion strategy is needed before the test can be used routinely and fully reliable mechanical behavior information can be derived from such tests.

Acknowledgments

The research performed at MIT has been supported by the Office of Fusion Energy, U.S. Department of Energy, under Contract DE-AC02-78ER-10107, that at Battelle by Battelle's Columbus Laboratories. The major portion of the research reported in this paper was performed by M. P. Manahan at MIT. We are grateful for the advice and assistance of Professor D. M. Parks of MIT in the use of the ABAQUS code. Professor N. J. Grant of MIT provided useful technical advice and some of the materials used in our tests. The authors appreciate the assistance of Dr. M. Lee and G. Kohse. The Hanford Engineering Development Laboratory provided the N-lot 316 SS used for most of the benchmark type tests reported here. The MDBT apparatus was skillfully machined by the craftsmen of the MIT Nuclear Reactor Laboratory.

References

[*1*] Manahan, M. P., "The Development of a Miniaturized Disk Bend Test for the Determination of Post-Irradiation Mechanical Behavior," Sc.D. thesis, Massachusetts Institute for Technology, Cambridge, Mass., 1982.

[*2*] Manahan, M. P., Argon, A. S., and Harling, O. K., "The Development of a Miniaturized Disk Bend Test for the Determination of Post-Irradiation Mechanical Properties," *Journal of Nuclear Materials*, Vol. 103 and 104, 1981, pp. 1545-1550.

[*3*] Manahan, M. P., Argon, A. S., and Harling, O. K., "Mechanical Behavior Evaluation Using the Miniaturized Disk Bend Test," Sixteenth Quarterly Technical Progress Report on Damage and Fundamental Studies, DOE/ER-0046/8, Oct.-Dec. 1981.

[*4*] Manahan, M. P., "A New Post-Irradiation Mechanical Behavior Test—The Miniaturized Disk Bend Test," invited paper at the American Nuclear Society 1982 Winter Meeting, 17 Nov. 1982, Washington, D.C.; published in *Journal of Nuclear Technology*, Vol. 63, No. 2, Nov. 1983.

[*4a*] Harling, O. K., Lee, M., Sohn, D-S, Kohse, G., and Lau, C. W. "The MIT Miniaturized Disk Bend Test," this publication, pp. 50-65.

[*5*] Annual Report on Alloy Development for Irradiation Performance in Fusion Reactors," Report MITNRL-003, 1978-1979.

[*6*] Szirmae, A. and Fisher, R. M., "Specimen Damage During Cutting and Grinding," in *Techniques of Electron Microscopy, Diffraction, and Microprobe Analysis, ASTM STP 372*, American Society for Testing and Materials, Philadelphia, 1965.

[*7*] Metallurgists to Industry, "Metallurgical Examination of EDM Cemented Carbide Samples," Report 47717, 27 Oct. 1982; available from Agietron Corp., P.O. Box 469, 839 South Route 53, Addison, IL 60101.

[*8*] Gettleman, K., Ed., "Wire EDM Challenges Aerospace," *Modern Machine Shop*, Oct. 1982.

[*9*] Paxton, M. M., "Mechanical Properties of Prototypic FTR Cladding—20% C.W. 316 Stainless Steel Tubing," HEDL-TME 71-59, Hanford Engineering Development Laboratory, Richland, Wash., April 1971.

[*10*] Dooley, M., Lucas, G. E., and Sheckherd, J. W., "Small Scale Ductility Tests," presented at Second Topical Meeting on Fusion Reactor Materials, 9-12 Aug. 1981, Seattle, Wash., and to be published in a special topical report of the *Journal of Nuclear Materials*.

[*11*] Hibbitt, H. D., Karlsson, B. I., and Sorenson, E. P., "ABAQUS: A General Purpose Finite Element Code," developed by Hibbitt, Karlsson, and Sorenson, Inc., Providence, R.I., Oct. 1982.

[*12*] Rodal, J. J. A., "Finite-Element Large-Deflection Finite-Strain Elastic-Plastic Transient Response Analysis of Structures," Ph.D. thesis, Massachusetts Institute of Technology, Cambridge, Mass., June 1979.

[13] Rabinowicz, E., *Friction and Wear of Materials,* Wiley, New York, 1965.
[14] Fish, R. L., Cannon, N. S., and Wire, G. L., "Tensile Property Correlations for Highly Irradiated 20 Percent Cold-Worked Type 316 Stainless Steel," in *Effects of Radiation on Structural Materials, ASTM STP 683,* J. A. Sprague and D. Kramer, Eds., American Society for Testing and Materials, Philadelphia, 1979, pp. 450-465.